

## New magnetic nano-absorbent for the determination of *n*-octanol/water partition coefficients

X. Gao<sup>a</sup>, C.H. Yu<sup>a</sup>, K.Y. Tam<sup>b</sup>, S.C. Tsang<sup>a,\*</sup>

<sup>a</sup> Surface and Catalysis Research Centre, School of Chemistry, University of Reading, Whiteknights, Reading RG6 6AD, UK

<sup>b</sup> AstraZeneca, Mereside, Alderley Park, Macclesfield, Cheshire SK10 4TG, UK

Received 3 June 2004; received in revised form 7 December 2004; accepted 10 December 2004

Available online 8 February 2005

### Abstract

A novel and generic miniaturization methodology for the determination of partition coefficient values of organic compounds in *n*-octanol/water by using magnetic nanoparticles is, for the first time, described. We have successfully designed, synthesised and characterised new colloidal stable porous silica-encapsulated magnetic nanoparticles of controlled dimensions. These nanoparticles absorbing a tiny amount of *n*-octanol in their porous silica over-layer are homogeneously dispersed into a bulk aqueous phase (pH 7.40) containing an organic compound prior to magnetic separation. The small size of the particles and the efficient mixing allow a rapid establishment of the partition equilibrium of the organic compound between the solid supported *n*-octanol nano-droplets and the bulk aqueous phase. UV–vis spectrophotometry is then applied as a quantitative method to determine the concentration of the organic compound in the aqueous phase both before and after partitioning (after magnetic separation).  $\log D$  values of organic compounds of pharmaceutical interest (0.65–3.50), determined by this novel methodology, were found to be in excellent agreement with the values measured by the shake-flask method in two independent laboratories, which are also consistent with the literature data. It was also found that this new technique gives a number of advantages such as providing an accurate measurement of  $\log D$  value, a much shorter experimental time and a smaller sample size required. With this approach, the formation of a problematic emulsion, commonly encountered in shake-flask experiments, is eliminated. It is envisaged that this method could be applicable to the high throughput  $\log D$  screening of drug candidates.

© 2005 Elsevier B.V. All rights reserved.

**Keywords:** Magnetic nanoparticle; Partition coefficient; Magnetic separation

### 1. Introduction

Lipophilicity is a very useful physicochemical parameter reflecting the transfer properties of a compound across biological membranes [1]. This can be described by the partition coefficient ( $\log D$ ), which is defined as the ratio of concentrations of a compound in all its forms between an aqueous phase (with buffer) and an oil phase. In particular, the *n*-octanol/water partition coefficient is commonly used in the pharmaceutical industry to reflect the lipophilicity of a potential drug compound [2,3]. Although there are some

theoretical approaches to assess lipophilicity of a chemical structure, their predictability for new chemical entities and/or novel structures is not satisfactory [4]. Consequently, an accurate measurement of the *n*-octanol/water partition coefficient using an appropriate methodology is essential in a drug evaluation programme.

The shake-flask method is a simple and traditional method for the determination of the  $\log D$  value [1,5]. It is accepted as a standard procedure by the Organisation for Economic Cooperation and Development (OECD) [6]. The compound is introduced into the two immiscible phases, *n*-octanol and aqueous buffer solution, in a separator funnel. The funnel is then shaken until the partitioning equilibrium is achieved. After phase separation, the concentration of the compound in each phase was determined. The drawbacks of this method include: a slow partitioning because of the bulk phases in-

\* Corresponding author. Tel.: +44 118 378 6346; fax: +44 118 378 6591.

E-mail addresses: [kin.tam@astrazeneca.com](mailto:kin.tam@astrazeneca.com) (K.Y. Tam), [s.c.e.tsang@reading.ac.uk](mailto:s.c.e.tsang@reading.ac.uk) (S.C. Tsang).

volved, it is labour intensive and emulsion formation upon shaking can interfere with the measurement. It has therefore been deemed unsuitable for a high throughput screening [7]. To overcome some of these problems, a stir-flask method has been developed. The vessel is gently stirred without shaking. However, a long period of time is employed (at least 36 h) in order to ensure the establishment of an equilibrium [8]. A chromatographic method using a column containing *n*-octanol-coated beads has also been reported [9–12]. The success of this approach depends very much on the quality of the calibration of the capacity factor against the log *D* values of standard compounds. Most often, this technique works well within a homologous series but it fails for structurally unrelated compounds. In addition, for ionised compounds, column-based techniques are not ideal, as the charged species are likely to coelute with the solvent front. Counter current chromatography (CCC) for log *D* measurements has then been developed [13]. In this method, the solute partitioning takes place between two immiscible solvents, one stationary and the other mobile. A gravitational or centrifugal force is utilised to hold the liquid stationary phase in the bed. CCC using centrifugal force for retaining the stationary phase is sometimes referred to as centrifugal partition chromatography (CPC). In these techniques, the log *D* value is determined from the retention volume ( $V_r$ ) of a solute (analyte) in relation to the stationary ( $V_s$ ) and mobile phase ( $V_m$ ) volumes based on the fundamental chromatographic relationship:  $V_r = D(V_s + V_m)$ . However, the main drawback of these techniques is that they are time-consuming and intensively hardware required [7,14]. A new method based on a flow injection extraction has recently been reported [15–17]. In this approach, the *n*-octanol and the compound containing aqueous buffer phases are segmented with each other in a specially designed manifold; from which the segmented stream then flows through an extraction coil for equilibration. Although it is a continuous system equipped with an on-line spectrophotometric detection, the method shows a narrow range of log *D* values [15–17]. More recently, Andersson and Schrader have proposed a dialysis tube method, which is claimed to capture compounds of a wider log *D* range [18]. But, this technique is rather complicated to set up and involves a long experimental time. As far as we are aware, all the above reported methods appear to suffer from either lacking of generality, simplicity, versatility, accuracy or more importantly, speed for a fast analysis to cope with the modern combinatorial synthesis of a large variety of compounds.

Hierarchical surfactant mediated assembly particularly on a magnetic body is a new emerging approach to the fabrication of functional nanometer-scale magnetic architectures [19]. We have recently synthesised new magnetic separable silica-coated iron oxide nanoparticles by a reverse microemulsion method, which can be dispersed in aqueous phase as a stable colloid. It has been shown that these nanoparticles are uniformly sized and possess super-paramagnetic properties [20]. In this particular application, we have used these porous nanoparticles for the physical storage of

*n*-octanol droplets for log *D* measurement with the aim of addressing the aforementioned drawbacks. Specifically, the composite nanoparticles are preloaded with a known amount of *n*-octanol dispersed into a bulk aqueous phase containing the analyte and buffer. The small *n*-octanol droplets on the nanoparticles create an excellent interface with the aqueous buffer phase, which significantly shortens the time required to achieve partition equilibrium. Thus, the super-paramagnetic properties of the nanoparticles allow a rapid magnetic induced phase separation followed by the analysis of the analyte in the bulk aqueous buffer phase by UV–vis spectrophotometry. Since the *n*-octanol is confined in silica over-layer, the formation of an emulsion, which is commonly encountered in shake-flask experiments, is virtually eliminated. We have also demonstrated that this novel method is capable of obtaining accurate log *D* values for selected compounds.

## 2. Materials and methods

### 2.1. Materials

Iron (II) chloride tetrahydrate, iron (III) chloride hexahydrate, potassium dihydrogenphosphate, tetraethyl orthosilicate (TEOS), cetyltrimethyl ammonium bromide (CTAB), *n*-Octanol (99%), 4-nitroanisole (97%), 4-nitrobenzyl alcohol (99%) and 4-nitrophenol (98%) were obtained from Aldrich. Imipramine, chlorpromazine, benzamide, 3,5-dichlorophenol and ibuprofen were obtained from Sigma. Quinoline (99%) and aniline (99.8%) were obtained from Fisher–Acros. Ammonia solution (35%) and toluene (>99%) were obtained from Fisher.

### 2.2. Methods

#### 2.2.1. Synthesis of porous silica-encapsulated nanoparticles

Porous silica-encapsulated magnetic nanoparticles as a nano-absorbent were synthesised using a modified microemulsion technique [20]. In the synthesis, a water:surfactant ratio ( $W_o$ ) of 20 was utilized. After the magnetic iron oxide core was obtained, TEOS was added to form the porous silica over-layer through the hydrolysis/condensation of the TEOS into silica gel in ammonia solution (high pH). The entire preparation was carried out in a nitrogen atmosphere. Characterisation of the nanoparticles were carried out using typical solid and surface characterisation techniques such as scanning electron microscopy (SEM), transmission electron microscopy (TEM), X-ray powder diffraction (XRD), energy dispersive spectrometry (EDS) and vibrating sample magnetometry (VSM). Detailed characterisation of particle dimensions, thickness of silica over-layers and chemical compositions of these nanoparticles can be found in our previous report [20].

### 2.2.2. *n*-Octanol absorption onto the nanoparticles

Prior to the loading of *n*-octanol, all samples were placed in a dynamic vacuum of  $6.5 \times 10^{-2}$  mbar at  $150^\circ\text{C}$  for at least 4 h in order to remove any volatile materials or solvent possibly trapped within the nanoparticles during the synthesis. We employed a gravimetric method to prepare the *n*-octanol filled nanoparticles. In a typical log *D* measurement experiment, 0.05 g nanoparticles were mixed with 0.0165 g *n*-octanol (since the density of *n*-octanol saturated with buffer was 0.824 g/ml hence 20  $\mu\text{l}$ , was therefore added) followed by adding 2.0 ml of aqueous drug solution ( $\sim 1 \times 10^{-5}$  M) in order to set the aqueous:*n*-octanol phase ratio to 100. It is noted that this amount of *n*-octanol is well below the maximum loading of *n*-octanol in the nanoparticles (0.54 ml/g determined by TGA experiment), thus no saturation of the *n*-octanol in the nanoparticles is ensured.

### 2.2.3. Buffer solution preparations

A buffer solution containing 10 mM potassium dihydrogen-phosphate was prepared using HPLC grade water. The pH of the buffer was adjusted by adding of appropriate amount of KOH solution to 7.40. The buffer was then placed in a 500 ml separatory funnel, 10 ml of *n*-octanol was added upon to allow the formation of a thin *n*-octanol layer above the aqueous phase. After shaking the funnel by hand for 5–10 min, the funnel was covered with aluminium foil and left for at least 3 days to ensure the two phases were mutually saturated. All the prepared solutions were stored in a cool and dry cupboard for further experiments.

### 2.2.4. Partition coefficient determination

**2.2.4.1. The partition experiment.** All the partition coefficient determination experiments were carried out in aqueous 10 mM potassium dihydrogen orthophosphate buffer, pre-saturated with *n*-octanol, at pH 7.40 at  $25^\circ\text{C}$ . An analyte was dissolved in this aqueous buffer solution at a concentration of about  $1 \times 10^{-5}$  M. The nanoparticles, preloaded with *n*-octanol, were allowed to disperse into the solution in a vial. The aqueous buffer phase:*n*-octanol ratio was adjusted to 100:1 unless otherwise stated. This vial was sealed and agitated in an orbital shaker for about 20 min. The shaking speed ( $\sim 80$  cycles per sec.) was carefully controlled to avoid any *n*-octanol droplets detaching from the particles. *n*-Octanol is lighter in weight than water due to its lower density. If it leaches from the nanoparticles, it would quickly rise up to the surface of the bulk aqueous phase and aggregate into small droplets or films. Thus, this crude but simple visual method could detect any *n*-octanol leaching from the nanoparticles. Magnetic induced precipitation of the nanoparticles was then achieved by using a permanent magnet ( $\text{BH}_{\text{max}} = 38 \text{ MGOe}$ ) situated at the bottom of the vial. UV–vis absorption spectra of the compound at the aqueous phase before and after partition were collected. All absorption data were background subtracted before used.

The log *D* value was calculated by the following equation:

$$\log D = \log \left\{ \left[ \frac{(A_1 - A_2)}{A_2} \right] \times \frac{V_w}{V_o} \right\} \quad (1)$$

where  $A_1$  and  $A_2$  represent the UV–vis absorption value of the compound at the aqueous phase before and after partition, respectively, while  $V_w/V_o$  represents the aqueous phase:*n*-octanol phase ratio.

For comparative purposes, the partition coefficients of all the compounds were independently measured by the shake-flask method at two laboratories (Reading and AstraZeneca). The aqueous phase:*n*-octanol ratio employed was kept the same (100) unless otherwise stated. Samples before and after partition were quantified by using UV–vis spectrophotometry (Reading) and a generic LC gradient coupled with UV detection (AstraZeneca) [21].

**2.2.4.2. The time required to achieve partition equilibrium.** To determine the time required in achieving partition equilibrium, the change of the UV–vis absorption value of a selected compound in the supernatant aqueous phase was monitored as a function of time. Two compounds, namely, 4-nitrobenzylalcohol ( $\lambda_{\text{max}} = 280 \text{ nm}$ ) and 4-nitroanisole ( $\lambda_{\text{max}} = 316 \text{ nm}$ ), were employed for this time analysis, respectively. Seven identical experiments, operated in a parallel manner, were carried out for each compound. The supernatants were then analyzed by UV–vis absorption after an exposure to an external magnetic field at the time intervals of 5, 10, 15, 20, 25, 30 and 60 min in turn (about 1 min is required to magnetically precipitate the colloid particles). The time-absorption changes were referenced to the aqueous solution containing the same compound but without adding the *n*-octanol filled nanoparticles ( $t = 0 \text{ min}$ ).

## 3. Results and discussion

### 3.1. Nanoparticles characterisation

XRD reveals that the average diameter of the iron oxide nanoparticles is 9.9 nm, which is in an excellent agreement with a value of 9.1 nm as shown from the TEM image in Fig. 1. It can be seen that the iron oxide formed as an inner core (darker fringe) is covered by several loosely packed silicon-oxygen containing over-layers, which appears to be amorphous and porous (see Fig. 1 with TEM images and a scheme of the particle). Energy dispersive spectrometry confirms that the elemental composition of these nanoparticles is  $\text{Fe}_3\text{O}_4 \cdot 1.74 \text{ SiO}_2$ . VSM analysis indicates that the saturation magnetisation per kilogram of the magnetic iron oxide core is of 76.16 emu/g. The value is close to the literature value of bulk  $\text{Fe}_3\text{O}_4$ , which is about 92 emu/g [22]. Also, the measured remanence of these nanoparticles is  $4.5 \text{ A m}^2/\text{kg}$  and coercivity is 15.3 k A/m. Magnetic remanence represents a magnetic field remained in material after it is exposed to an external magnetic field. The coercivity is defined as

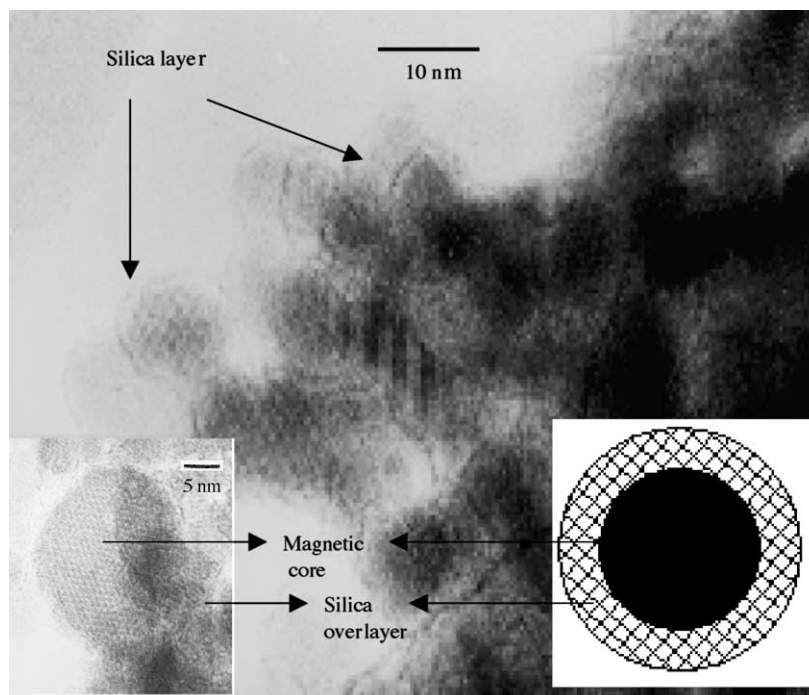


Fig. 1. TEM image and a model of the silica coated magnetic nanoparticles.

the magnetic property of a material, which resists its demagnetisation. High magnetic remanence and high coercivity values indicate that the material is a 'hard' type of magnetic material. Thus, our nanoparticles are characterized with low remanence and coercivity values suggest that the particles will only behave as little magnets upon exposure to a strong external magnetic field leading to precipitation. Without the magnetic field, the 'soft' nanoparticles will return as colloidal dispersed particles. Thus, these data clearly agree that the nanoparticles exhibit super-paramagnetic behavior at room temperature as expected from the nano-sized iron oxide particles. It is important to note that the super-paramagnetism means that there is no remaining induced magnetism due to repeated exposure of magnetic field.

### 3.2. Partition coefficient determination

Table 1 shows the average  $\log D$  values of some selected compounds determined by the nanoparticles method and the shake-flask method compared to the literature data. The quoted  $\log D$  value for each drug compound is an average value obtained by repetitive measurements for at least five times by both the nanoparticle method and the shake-flask method. Fig. 2 shows very small deviations of the average measured data for each sample compared with the data obtained from the standard shake-flask method and the literature. Linear regression analyses on the curves reveal correlation coefficients of greater than 0.98, with slopes and intercepts close to unity. This clearly suggests that the  $\log D$  values measured by the present nanoparticle method are in excellent agreement with those obtained

from the shake-flask method and the literature data. It also indicates the repeatability of the present method for the  $\log D$  measurement.

This is a concern that some polar drug compounds especially those generally known as strong hydrogen bond acceptor compounds, such as pyridine and quinoline, may selectively bind onto the OH groups on the silica surface. As

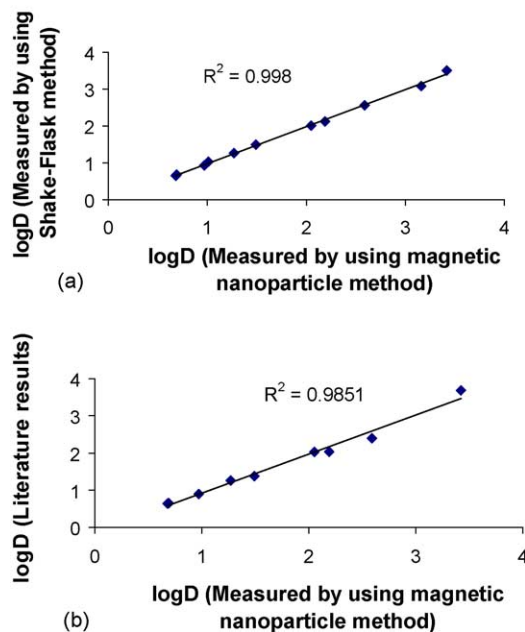
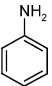
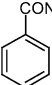
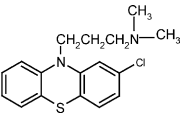
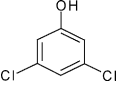
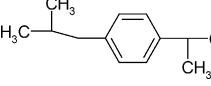
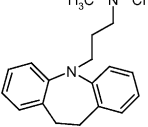
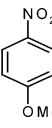
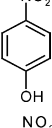
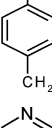
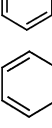
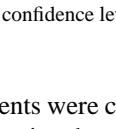


Fig. 2. The correlations of  $\log D$  values obtained by the present nanoparticle method with (a) a shake-flask method and (b) the literature value.

Table 1  
Partition coefficients ( $\log D$ ) of selected compounds as determined by the nanoparticles method and the shake-flask method in pH 7.4 at 25 °C<sup>a</sup>

| Compound             | Structure   | Nanoparticles   | Shake-flask |                 | Literature      |
|----------------------|---|---|-------------|-----------------|-----------------|
|                      |   |   | Reading     | AstraZeneca     |                 |
| Aniline              |    | 0.97 ± 0.03   | 0.93 ± 0.01 | NA <sup>b</sup> | 0.90 [23]       |
| Benzamide            |    | 0.68 ± 0.05   | 0.65 ± 0.01 | 0.66            | 0.64 [23]       |
| Chlorpromazine       |    | 3.16 ± 0.01, 3.18 ± 0.45 (aqueous phase: <i>n</i> -octanol = 890:1) | 3.08 ± 0.01 | 3.20            | NA <sup>b</sup> |
| 3,5-Dichlorophenol   |    | 3.42 ± 0.04   | 3.50 ± 0.05 | 3.56            | 3.68 [24]       |
| Ibuprofen            |    | 1.01 ± 0.06   | 1.03 ± 0.03 | 1.10            | NA <sup>b</sup> |
| Imipramine           |    | 2.59 ± 0.16   | 2.56 ± 0.04 | 2.50            | 2.40 [25]       |
| 4-Nitroanisole       |   | 2.01 ± 0.01, 2.05 ± 0.07 (aqueous phase: <i>n</i> -octanol = 890:1) | 2.01 ± 0.01 | NA <sup>b</sup> | 2.03 [23]       |
| 4-Nitrophenol        |  | 1.49 ± 0.02   | 1.49 ± 0.01 | 1.48            | 1.38 [26]       |
| 4-Nitrobenzylalcohol |  | 1.27 ± 0.04   | 1.26 ± 0.01 | NA <sup>b</sup> | 1.26 [23]       |
| Pyridine             |  | 0.69 ± 0.02   | 0.68 ± 0.02 | 0.66            | 0.65 [27]       |
| Quinoline            |  | 2.19 ± 0.01   | 2.12 ± 0.01 | 2.02            | 2.03 [27]       |

<sup>a</sup> Uncertainty at 95% confidence level determined from five repeated measurements.

<sup>b</sup> Not available.

a result, measurements were carried out on the nanoparticles with and without capping the surface silanol groups (Table 2). As noted from the table, no significant difference of the  $\log D$  values was obtained with and without the capping treatments.

It is especially noted that the magnetic induced separation (precipitation) of the particles from the supernatant can be accomplished within 1 min. Fig. 3 shows the typical UV–vis absorbance changes of 4-nitrobenzylalcohol and 4-nitroanisole in the supernatant buffer phase (measured after the separation) as a function of time. The data indicates that a partition

Table 2  
Partition coefficients ( $\log D$ ) of selected hydrogen bond acceptor compounds with and without removal of surface silanol groups

| Compound       | $\log D$ (nanoparticles with free —OH) | $\log D$ (nanoparticles with —OH capped by chlorotrimethylsilane (CTMS <sup>a</sup> )) |
|----------------|--|--|
| Aniline        | 0.973                                  | 0.968  |
| Quinoline      | 2.186                                  | 2.181  |
| Chlorpromazine | 3.164                                  | 3.170  |

<sup>a</sup> Excess CTMS was mixed with nanoparticles at 55 °C.

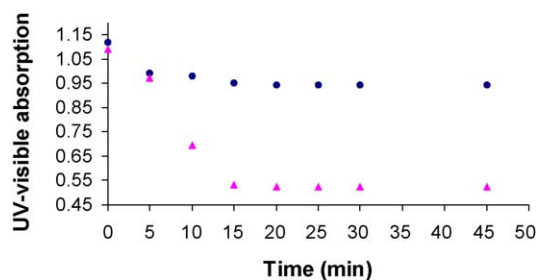


Fig. 3. The change of UV–vis absorptions of 4-nitrobenzylalcohol and 4-nitroanisole in aqueous supernatant phase as a function of time after the magnetic induced precipitation of the nanoparticles.

equilibration time of <15 min is required for both of the compounds (including the time for the magnetic precipitation), which is much shorter than many reported methods [7,18]. This may suggest that the *n*-octanol is likely to be absorbed by the nanoparticles in form of very small droplets. Consequently, the interfacial contact between the aqueous and the *n*-octanol phases is far higher than that of the traditional shake-flask experiment for the rapid establishment of equilibrium. In contrast, it is well accepted that the traditional shake-flask requires a much longer experiment time (>12 h) as the inter-dispersed emulsion droplets would require a long time to settle (despite the fact that improved modern designs can substantially reduce the analytical time to be within a few hours).

In addition, it is anticipated that the present method would be useful for the determination of high  $\log D$  compounds, which would be useful in drug discovery. High  $\log D$  value implies that the compound is very soluble in *n*-octanol, so leaving very low concentrations in the aqueous phase after partition which may well fall below the detection limit of the analytical technique used. By reducing the amount of *n*-octanol, the concentration of the compound after partition may become quantifiable (see Eq. (1)). However, it is rather difficult to achieve this in shake-flask method since a visual distinction of the two immiscible phases has to be maintained. As a result, a large quantity of solvents and compounds, are therefore required. On the other hand, in our case, reduction of sample volume can be achieved easily by reducing the amount of nanoparticles dispersed in the aqueous phase. To illustrate this point, it can be seen from Table 1 that an extremely large aqueous phase:*n*-octanol phase ratio (890:1) can be achieved by using the nanoparticles as the *n*-octanol carrier. It should be borne in mind that this could not be easily established using the shake-flask method in a small flask. However, further widening the present  $\log D$  range shown in Table 1 (such as using bifonazole,  $\log D = 4.77$ ) was not successful. This is attributed to the extremely low solubility of these compounds in aqueous phase and the limited sensitivity of the UV–vis spectrometry. The problem could be resolved by using more sensitive techniques such as LC–MS, which will be evaluated in the future. As a result, a  $\log D$  range of 0.65–3.50 is now demonstrated by this method. This range, however, is still not yet capable of capturing pharmaceutical compounds with

high  $\log D$  values. As a result, further improvement in the  $\log D$  range is required. Nevertheless, it is believed that the novel procedure described here could offer a robotic friendly miniaturization platform, which would be well adopted as an automation method for a high throughput  $\log D$  screen of drug candidates.

#### 4. Conclusion

A novel methodology in tailoring porous silica-encapsulated iron oxide nanoparticles to determine the partition coefficient of organic compounds in aqueous phase/*n*-octanol has been developed. Our experimental results clearly demonstrate the usefulness of this novel method for the actual determination of partition coefficient values, which requires only a very small quantity of compound, solvent and the nanoparticles. It was found that the  $\log D$  values as measured by this novel method were in excellent agreement with those determined by the shake-flask method at two different laboratories and correlated extremely well with literature values where available. We have demonstrated that this novel but direct method can circumvent some current problems in  $\log D$  determination using other methods, such as long analysis time, cumbersome, labor intensive and undesirable emulsion formation.

#### Acknowledgements

This manuscript is dedicated to Late Mr. Alan Wait of AstraZeneca (AZ) who significantly contributed some very useful discussions to this work. XG would like to acknowledge his Ph.D. studentship from the AZ.

#### References

- [1] J. Comer, K. Tam, in: B. Testa, H.V. de Waterbeemd, G. Folkers, R. Guy (Eds.), *Pharmacokinetic Optimisation in Drug Research*, Wiley-VCH, Weinheim, 2001, Chapter 17.
- [2] A. Leo, C. Hansch, C. Church, *J. Med. Chem.* 12 (1969) 766–771.
- [3] C. Hansch, T. Fujita, *J. Am. Chem. Soc.* 86 (1964) 1616–1626.
- [4] P. Bruneau, J. Morris, in: H.J. Bohm, G. Schneider (Eds.), *Virtual Screening for Bioactive Molecules*, Wiley-VCH, Chichester, 2000, Chapter 3.
- [5] J. Oprea, A.M. Davis, S.J. Teague, P.D. Leeson, *J. Chem. Inf. Comput. Sci.* 41 (2001) 1308–1315.
- [6] OECD, *Guidelines for Testing of Chemicals*, OECD, Paris, 1992 (No. 107).
- [7] L.G. Danielsson, Y.H. Zhang, *Trends Anal. Chem.* 15 (1996) 188–196.
- [8] J. de Bruijn, F. Busser, W. Seinen, J. Hermens, *Environ. Toxicol. Chem.* 8 (1989) 499–512.
- [9] P.A. Rapaport, S.J. Eisenreich, *Environ. Sci. Technol.* 18 (1984) 163–170.
- [10] M. Hsieh, J.G. Dorsey, *Anal. Chem.* 67 (1995) 48–57.
- [11] K. Valkó, C. Bevan, D. Reynolds, *Anal. Chem.* 69 (1997) 2022–2029.

- [12] B. Dimitrova, I. Doytchinova, M. Zlatkova, *J. Pharm. Bio. Anal.* 23 (2000) 955–964.
- [13] A.P. Foucault, *Anal. Chem.* 63 (1991) 569A–579A.
- [14] B.J. Herbert, J.G. Dorsey, *Anal. Chem.* 67 (1995) 744–749.
- [15] V. Kuban, *Anal. Chim. Acta* 248 (1991) 493–499.
- [16] V. Kuban, L.G. Danielsson, F. Ingman, *Anal. Chem.* 62 (1990) 2026–2032.
- [17] A.G. Howard, C.Y. Yeh, *Anal. Chem.* 70 (1998) 4868–4872.
- [18] J.T. Andersson, W. Schrader, *Anal. Chem.* 71 (1999) 3610–3614.
- [19] S. Santra, R. Tapeç, N. Theodoropoulou, J. Dobson, A. Hebard, W.H. Tan, *Langmuir* 17 (2001) 2900–2906.
- [20] X. Gao, K.M.Y. Yu, K.Y. Tam, S.C. Tsang, *Chem. Commun.* 24 (2003) 2998–2999.
- [21] B. Law, D. Temesi, *J. Chromatogr. B* 748 (2000) 21–30.
- [22] C.B. de Boer, M.J. Dekkers, *Geophys. J. Int.* 133 (1998) 541–552.
- [23] T. Fujita, J. Iwasa, C. Hansch, *J. Am. Chem. Soc.* 86 (1964) 5175–5180.
- [24] F. Lombardo, M.Y. Shalaeva, K.A. Tupper, F. Gao, *J. Med. Chem.* 44 (2001) 2490–2506.
- [25] C. Hansch, A.J. Leo, *Substituent Constants for Correlation Analysis in Chemistry and Biology*, Wiley, New York, 1979.
- [26] H. Illing, D. Benford, *Biochem. Biophys. Acta* 429 (1976) 768–779.
- [27] J. Iwasa, T. Fujita, C. Hansch, *J. Med. Chem.* 8 (1965) 150–153.